Hydrophobic Tendency of Polar Group Hydration as a Major Force in Type I Antifreeze Protein Recognition

Cheng Yang and Kim A. Sharp*
E.R. Johnson Research Foundation, Department of Biochemistry and Biophysics, University of Pennsylvania, Philadelphia, Pennsylvania

ABSTRACT The random network model of water quantitatively describes the different hydration heat capacities of polar and apolar solutes in terms of distortions of the water–water hydrogen bonding angle in the first hydration shell (Gallagher and Sharp, JACS 2003;125:9853). The distribution of this angle in pure water is bimodal, with a low-angle population and high-angle population. Polar solutes increase the high-angle population while apolar solutes increase the low-angle population. The ratio of the two populations quantifies the hydrophobicity of the solute and provides a sensitive measure of water structural distortions. This method of analysis is applied to study hydration of type I thermal hysteresis protein (THP) from winter flounder and three quadruple mutants of four threonine residues at positions 2, 13, 24, and 35. Wild-type and two mutants (VVVV and AAAA) have antifreeze (thermal hysteresis) activity, while the other mutant (SSSS) has no activity. The analysis reveals significant differences in the hydration structure of the ice-binding site. For the SSSS mutant, polar groups have a typical polar-like hydration, that is, more high-angle H-bonds than bulk water. For the wild-type and active mutants, polar groups have unusual, very apolar-like hydration, that is, more low-angle H-bonds than bulk water. This pattern of hydration was seen previously in the structurally distinct type III THPs (Yang & Sharp Biophys Chem 2004;109:137), suggesting for the first time a general mechanism for different THP classes. The specific shape, residue size, and clustering of both polar and apoler groups are essential for an active ice binding surface. Proteins 2005;59:266–274.
© 2005 Wiley-Liss, Inc.

Key words: solvation; random network model; thermal hysteresis protein; water structure; polarity

INTRODUCTION

Antifreeze or thermal hysteresis proteins (THP) have been found in a variety of organisms, including fish, spiders, insects, and bacteria. These proteins are able to depress the freezing point of aqueous solutions by adsorbing to ice crystal nuclei and inhibiting their growth in solution. THPs lower the freezing point of a solution without changing the melting point. The difference between the freezing and the melting point is termed thermal hysteresis (TH), which is widely used as an indicator of THP activity. Three of five structurally diverse fish THPs have been determined by X-ray and NMR techniques, including type I THP from winter flounder,[1] type II THP from sea raven,[2] and type III THP from eel pout.[3] The type I THP is a single, slightly curved alpha-helical peptide that contains three 11 amino acid repeats of Thr-X2-Asx-X7, where X is generally alanine.[1] Its ice-binding site has been recently defined as the conserved Thr-Ala-Ala-Thr motif.[4] However, the precise mechanism by which THPs bind to ice crystals and inhibit ice growth is still unclear. Many questions remain regarding the mechanism of specificity and affinity in these proteins. This includes the crucial question of how THPs can use either polar or apolar groups to recognize ice crystals forming in a large excess of liquid water and how water molecules are structured on the protein's binding surface. If the protein uses polar groups to recognize ice, then ordinarily such groups will have a higher affinity for liquid water (which is more distorted, and better able to electrostatically solvate the group), which is present at large excess (55 M). So net binding to ice, present initially at low concentrations, will be negligible, that is, specificity will be low. On the other hand, if the protein uses apolar groups, they normally prefer more ice-like water in their hydration shell, but their affinity for any kind of water, liquid or ice, is low because they only make weak van der Waals interactions. This creates an apparent affinity/specificity dilemma in terms of choosing groups to construct a specific ice nucleus binding surface.

No general mechanism, by which all THPs associate with ice crystals and stop their growth, has been proposed. Three models have been proposed for type I alpha-helical THP. The first is based on a lattice match of ice oxygen atoms with hydrogen-bonding groups on the protein.[5,6] In contrast, the second model emphasized the role of the hydrophobic part of type I THPs in binding to ice surface.[7–11] The third model, a dynamic version of the first model, proposed the effect of initial association of one repeat unit of the helix with ice crystal on the subsequent

binding of other repeat units through "remodeling" of the ice surface.[12] Moreover, none of these models may apply to type III THPs because they lack many structural features of type I THPs, notably the 11-residue Thr-repeat structural motif. To explain type III THPs activity, a model based on an alignment of five hydrogen-bonding atoms on the putative ice-binding face and ice oxygen atoms on the prism plane was proposed.[3,13] A subsequent study indicated that side-chain orientation and tight packing limit the formation of possible hydrogen bonds and concluded that hydrophobic groups on ice-binding site might play an important role in protein–ice interaction.[14] A computer simulation also emphasized the necessity for a favorable orientation that maximizes hydrogen bond and van der Waals interactions.[15] A neural network study, based on calculation of contributions from the accessible surface area of a protein, as well as hydrophobic, polar, and charged residues, predicted that a certain level of hydrophobicity in ice-binding site is essential for type III THP activity.[16] A computational study also found a contribution to THP activity from hydrophobic residues on the periphery of putative ice-binding site.[17]

Previously, we developed a quantitative analysis of changes in water structure induced by polar and apolar solutes based on the random network model (RNM),[18] which characterizes changes in the water–water angle distribution function[19–22] The main features of solute-induced water structure revealed by this analysis are: the water–water angle distribution function of pure water is bimodal with a low-angle population and a high-angle population, center at approximately 12 degrees and approximately 54 degrees, respectively. Solutes perturb the structure of water principally in their first hydration shell by changing the ratio of these two populations, apolar solutes increasing the low-angle population, polar solutes increasing the high-angle population. The ratio of these two populations may represent quantitatively the hydrophobicity of water. There is a direct link between these angular structural changes in the water hydrogen bond network in the first hydration shell of solute and heat capacity changes. A combination of explicit water simulations and this RNM analysis yields a quantitative agreement between measured and calculated hydration heat capacities, as well as a revealing description of the change in water structure induced by apolar and polar solutes.

We recently applied the RNM method of analysis of water hydration to Type III THP from eel pout.[22,23] The wild-type protein and three point mutants were studied. Residue A16 in the middle of the ice-binding site was replaced by either cystine, retaining thermal hysteresis activity, or by threonine or tyrosine, which destroyed activity. The analysis revealed significant differences in the hydration structure of the ice-binding site (centered on residue 16) among four proteins. For the A16T and A16Y mutants with reduced activity, polar groups had a typical polar-like hydration, that is, more high-angle H-bonds than bulk water. For the wild-type and mutant A16C with 100% of the wild-type activity, polar groups have unusual, very apolar-like hydration, that is, more low-angle H-

bonds than bulk water. The water around the active ice-binding site, in addition to having a more ice-like pattern of hydrogen bonding on the ice-binding face, was also more structurally homogeneous. In contrast, for the A16T and A16Y mutants the water–water H-bonds are more distorted and the structure more heterogenous. Overall, the binding surface of the active proteins strongly enhanced the water tetrahedral structure, taht is, promoted ice-like hydration. The unique pattern of hydration around the polar groups was found only in the active ice-binding region, and nowhere else on either the inactive proteins, or the nonice-binding regions of the active proteins. It was concluded that the specific shape, residue size, and clustering of both polar/apolar groups were essential for the binding surface to recognize, and preferentially interact with nascent ice crystals forming in liquid water.

To better understand the structure–function relationship of type I THP, we apply the same type of water–water angle distribution function analysis to study the hydration structure of wild- type and three quadruple mutants at the positions of 2, 13, 24, and 35: The (T2A + T13A + T24A + T35A) quadruple mutant, denoted AAAA mutant, the (T2S + T13S + T24S + T35S) quadruple mutant denoted by SSSS mutant, and the (T2V + T13V + T24V + T35V) quadruple mutant denoted by VVVV. Two specific questions we address are: (1) whether there are significant differences in hydration structures among wild-type and three mutants, (2) whether this analysis can shed light on the mechanism of type I THPs activity.

METHODS
Molecular Dynamics Simulations

Type I antifreeze wild-type and three quadruple mutants were selected due to their different thermal hysteresis (TH) activity and the structural characteristics of the side chains of mutated residues. The AAAA and VVVV mutants have TH activity, while the SSSS mutant has no TH activity. The starting coordinate of the wild type was taken from Protein Data Bank (PDB entry 1WFA[1]). Three quadruple mutants were built from the wild-type structure by replacing four Thr residues at the positions of 2, 13, 24, and 35 with four Ala, four Ser, and four Val, respectively, using Insight (Accelerys, San Diego, CA). CHARMM[24,25] was used to build the hydrogen atoms needed in the all-atom model, and the positions of the mutated residues in each mutant were energy-minimized with the rest of the protein was kept fixed. The wild-type structure is shown in Figure 1, with the binding face of the helix oriented up, and the threonine residues shown in CPK. Each protein was placed in a 74 Å × 40 Å × 40 Å rectangular box of TIP3P water molecules. The water molecules that overlapped with the protein were eliminated. Each final simulation system consists of approximately 19,966 atoms including about 6672 water molecules, providing at least five layers of solvating water.

All molecular dynamics (MD) simulations were performed using the program CHARMM. For each protein, the whole system was first briefly energy minimized (200
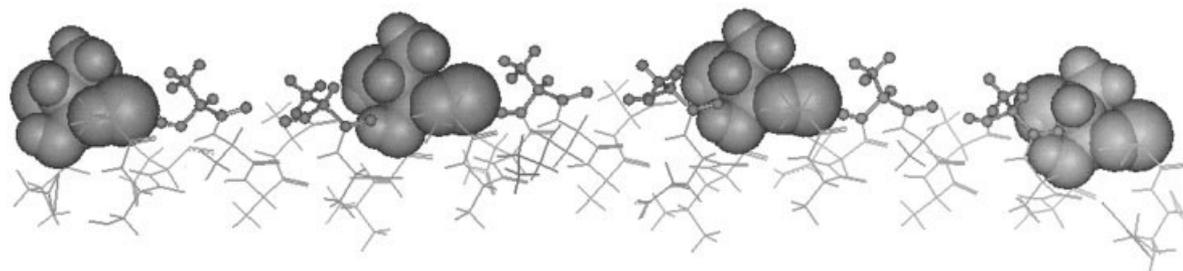
Fig. 1.   The crystal structure of type I THP (PDB entry: 1WFA). The ice-binding face is on the top, including three 11-amino acid repetitive units along the helix. Thr 2, Thr 13, Thr 24, and Thr 35 on the ice-binding surface are shown in CPK representation. Ala 6, 10, 17, 21, 28, and 32 on the ice-binding surface are shown in ball-and-stick representation.
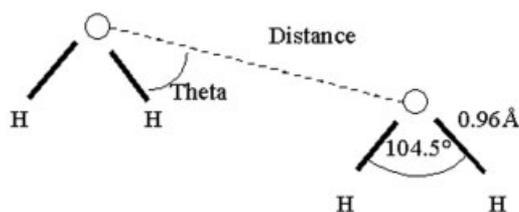

Fig. 2.   Water structure. The geometry of the TIP3P water is shown. The water–water distance is taken as the distance between O atoms. The water–water angle is defined as the minimum of the four HO–O angles. Note that given the TIP3P HOH angle of 104.5°, the maximum possible value of theta is $(180 - 104.5°/2) = 127.8°$.

steps of adaptive basis Newton-Raphson minimization) and then equilibrated over a period of 50 ps. Finally, a 1-ns MD trajectory was generated. The equilibration and trajectory generation were performed by MD using the leapfrog algorithm with a time step of 2 fs, at a constant temperature of 300 K and constant pressure of 1 atm. The Nose-Hoover method was used to maintain constant temperature and the Langevin piston method for constant pressure. Minimum image periodic boundary conditions were employed. In all computations SHAKE constraints were used to fix the lengths of the bonds involving hydrogen atoms. Electrostatic and van der Waals interactions were truncated using a shifting function between 10.0 and 12.0 Å.

Water–Water Angular Distribution Function

Snapshots of the water–protein trajectory were saved every 100 fs for analysis using the program PRAM,[26] which uses CHARMM trajectory files as input. The first hydration shell waters were identified by finding all waters within the first hydration shell cutoff of any protein atom. The first shell hydration cutoff for each atom type is defined as the first minimum in the atom–water radial distribution function g(r). The g(r) for each atom type was previously obtained from preliminary simulations on the model compounds alanine dipeptide and cysteine dipeptide, which contain all the required atom types.[26] Every pair of waters within a water–water distance cutoff was then analyzed, the distance r and angle *theta* being defined as in Figure 2. A water–water angular distribution function P(theta) is then obtained. A water–water distance cutoff of 4.0 Å was employed, due to its sensitivity in

describing hydration heat capacity of polar and apolar solutes,[27] and for consistency with our previous analyses.[23,26] It is common to define an H-bond for heavy-atom separations significantly less than 4.0 Å (usually in the range 2.9–3.4 Å), and often an angle cutoff is applied as well. However, for conciseness, we shall refer hereafter to *theta* as the H-bond angle for any configuration of a water pair within 4 Å. This also recognizes the fact that water structure variables vary continuously.

Water–water P(theta) distributions were also subclassified based on the type of protein atoms being hydrated. All atoms in the protein were first classified as being apolar, polar, or weakly polar, based on the partial charge assigned by the molecular dynamics force field. Those atoms possessing a charge magnitude less than 0.35 are considered apolar, charge magnitude 0.35–0.45 are classified as weakly polar, and atoms with a partial charge magnitude greater than 0.45 are considered polar. Solute atoms of interest can also be "tagged" before analyzing the trajectory, allowing the hydration structure of subsets of the protein surface to be examined. Water–Water P(theta) distributions were calculated separately for the three possible combinations of solute atom polarity class: polar–polar, apolar–apolar, and polar–apolar (mixed). For example, if the first water oxygen was closest to an apolar solute atom and the second water oxygen was closest to a polar solute atom, that water–water angle would be added to the mixed angle frequency histogram.

Analysis of Angle Probability Distributions

To obtain a quantitative comparison of P(theta) curves, the area under each peak, corresponding to the populations of low-angle and high-angle water–water geometry, was obtained by numerical integration using the trapezoidal rule as implemented in Origin 6.0 (Microcal). The ratio of these two areas is characteristic of the type of solute (apolar, polar, etc.). Reference ratios were calculated from simulations of several small molecules of differing polarity studied previously using the RNM-explicit water method.[19–22] Thus, we may interpret the distribution of water–water angles surrounding the protein surface in relation to small test solutes of known polarity.

Surface Subsets and Controls

The hydration structure of the entire type I THP surface was evaluated according to the procedures outline above.
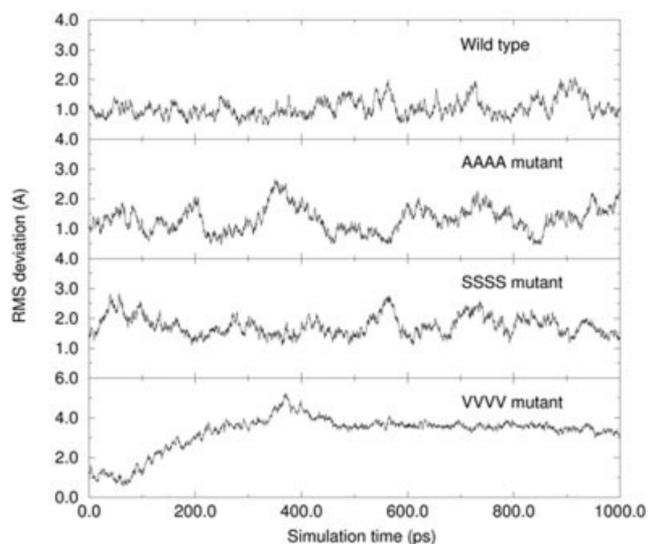
Fig. 3. Simulation convergence behavior, plotted as RMS deviation in atomic coordinates from the starting structures as a function of simulation time.
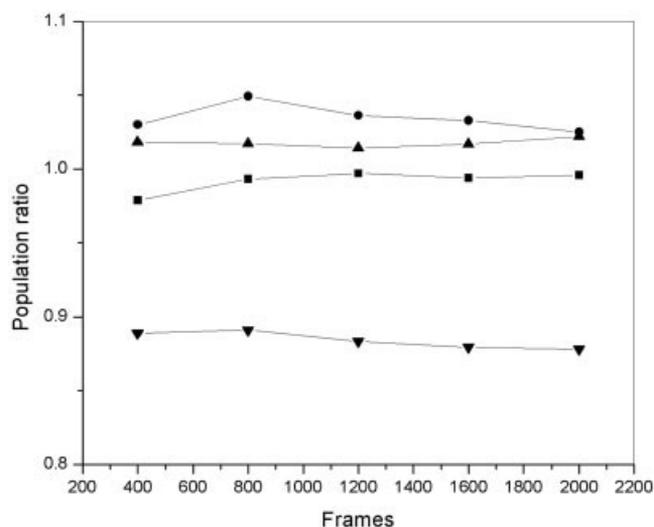

Fig. 4. Evolution of low-angle/high-angle population ratios for the ice-binding sites of wild-type and SSSS mutant. The ratios are shown as a function of the number of configurations analyzed. Hydrating water–water class: (■) apolar, wild-type, (●) polar, wild-type; (▲) apolar, SSSS mutant, (▼) polar, SSSS mutant.

We also examined several subsets of the protein surface. These included the ice-binding unit that is composed of residues 13, 17, 21, and 24. We also analyzed the hydration structure surrounding the residues of 13 and 24.

RESULTS

The convergence of the simulations was monitored by plotting the root-mean-squared (RMS) deviation of atomic coordinates from the starting structures as a function of simulation time, shown in Figure 3. For wild-type, AAAA, and SSSS mutants, the results show stable well-converged simulations throughout 1-ns trajectories with modest deviations. For the VVVV mutant, convergence was somewhat slower, but the RMS deviation indicated a stable simulation during the last 600 ps of the trajectory. In addition, we monitored the convergence of the specific structural parameter of interest, the P(theta) distribution, and the angle population ratio. The time evolution of selected high H-bond angle/low-angle ratios are shown in Figure 4. These are typical, and show rapid convergence of the angle distribution population ratio, whose analysis we focus on here.

Overall P(theta) Distributions for Type I THP

The water–water angle distributions for the entire first hydration shell of type I THPs are shown in Figure 5, and are typical of the profiles seen for the different classes of water pairs solvating small molecules.[19–22] The apolar–apolar pairs have a higher fraction of the low-angle population, while the polar–polar pairs have a higher fraction of the high-angle population. The water–water angle distribution for pure water is shown for comparison. Population ratios are summarized in Figure 8. The characteristic small molecules (methane, potassium, pure water) are included as the points of reference, and are indicated by the horizontal lines on the histogram. For four proteins,

the low/high-angle population ratios of apolar atoms are larger than that of pure water, while those of polar atoms are smaller than that of pure water. In general, overall water–water angle distributions for wild-type and three mutants are very similar. Thus, overall water structures around four proteins are similar.

P(theta) Distributions for Type I THP Ice-Binding Sites

Type I THP from winter flounder is an alanine-rich, 37-amino acid, single alpha-helix that contains three 11 residue repeats. Its ice-binding site has been defined as the Ala-rich face of the helix, which involves Thr-13, Ala-17, and Ala-21, and equivalent residues at 11 amino acid intervals along the helix.[4] To explain the mechanism of type I THPs activity, we analyzed the water structure around one repetitive unit of the ice-binding face, which is comprised of residues 13, 17, 21, and 24. The P(theta) distributions for wild-type and three mutants are shown in Figure 6. Their population ratios are summarized in Figure 8.

Two main features are noted for the hydration of type I THP ice-binding surfaces, compared to the average hydration structure over the entire surface. First, both polar and apolar groups on the ice-binding face have larger low- to high-angle population ratios than those for the entire protein surface. This is true for wild-type and the three mutants, which demonstrates their ice-binding surfaces are more hydrophobic on average. For example, in wild-type protein the population ratio for apolar groups on the ice-binding site is 0.98, 13% larger than the entire protein surface (0.87). Second, the hydration on the ice-binding surface displays a significant difference between active and inactive proteins. This is in contrast to the average hydration over the entire surface, which shows no qualitative difference between active and inactive proteins.
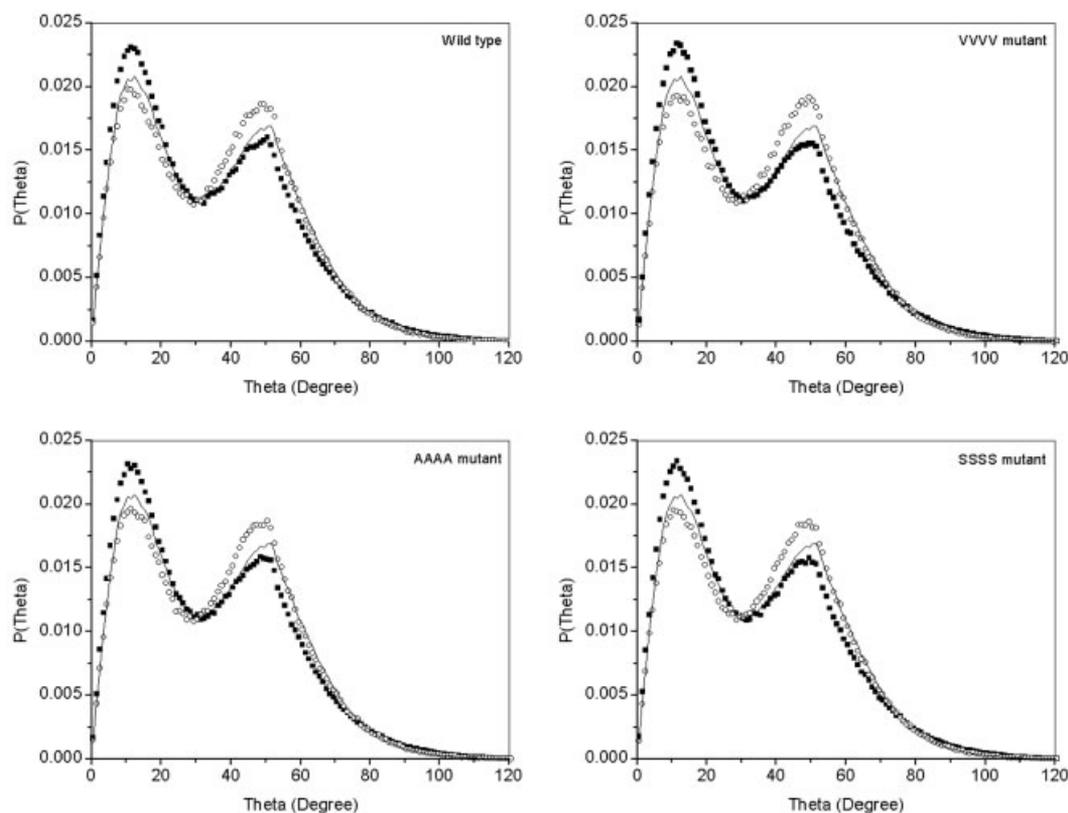
Fig. 5.   Overall water structure around type I THPs. The water–water angle probability distributions for the first hydration shell of the wild-type and three quadruple mutant proteins. Hydrating water–water class: (■) apolar, (○) polar, (—) pure water.

The most striking feature is that in the ice-binding site the fraction of the low-angle population around polar groups is larger than that around apolar groups for the wild-type, active AAAA and VVVV mutants. This comes primarily from a large shift in the angular distribution of polar-type water pairs towards that of apolar-type (low H-bond angle) water pairs in the ice-binding site, indicating two things: (1) a less distorted, more tetrahedral or hydrophobic-like water structuring around the ice-binding site; (2) a more homogenous or uniform hydration structure in the ice-binding site, that is, less structural variation around the polar versus apolar groups.

In contrast to wild-type and two active mutants, the inactive SSSS mutant displays the standard water structure around polar and apolar groups in the ice-binding site, that is, more high-angle H-bonds around the former, more low-angle H-bonds around the latter, and a consequent heterogeneous hydration structure. These changes are apparent in the summary of population ratios in Figure 8, where the significant changes for the ice-binding site are in the population ratio for polar groups. For wild-type, the low- to high-angle population ratio is 1.03 around polar groups, 3% *greater* than that for apolar groups in the ice-binding site (1.00). However, for the SSSS mutant the ratio around polar groups is 0.88, 16% *less* than that for apolar groups in the ice-binding site (1.02). This difference indicates that there is some relation-

ship between the hydration structure on the ice-binding face and thermal hysteresis activity.

Water Structure Surrounding the Key Residues of the Ice-Binding Site

To understand the effect of the side chains of mutated residues on type I THP activity, the hydration in the immediate vicinity of the key residues 13 and 24 in the ice-binding site was further analyzed in the wild-type and three mutants. Their P(theta) distributions are shown in Figure 7, and their population ratios are summarized in Figure 8. There is a significant difference in water–water angular distributions between active and inactive proteins. The fraction of the low-angle population around polar groups in residues 13 and 24 of the ice-binding site is the same as or larger than that around apolar groups for wild-type and active AAAA and VVVV mutants. The large shift to low angles in their P(theta) distributions for the polar hydrating water class indicates a significant increase in more tetrahedral-like water pairs and a more uniform hydration structure across the polar and apolar groups. In contrast, the inactive SSSS mutant displays "standard" water structure differences between the apolar and polar groups of residues 13 and 24 in the ice-binding site. Again, the systematic and qualitative difference between active and inactive proteins implies some relationship between the hydration structure around these residues of the
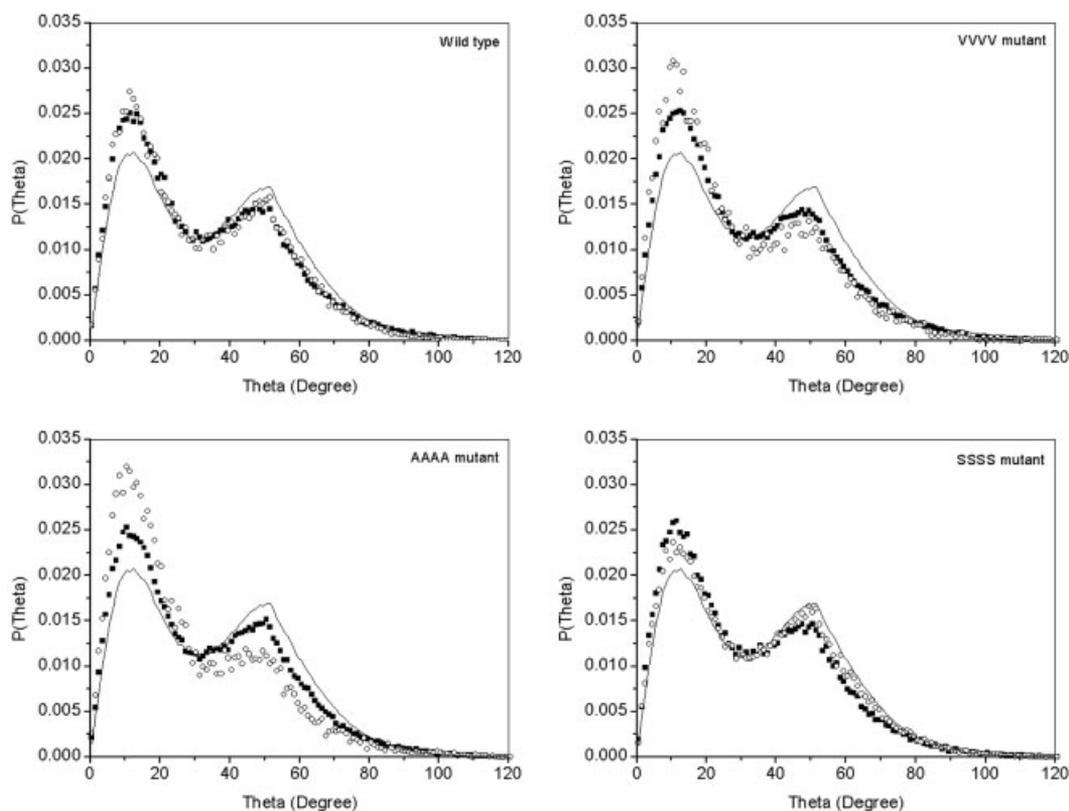
Fig. 6. Water structure around type I THPs ice-binding sites. The water–water angle probability distributions for the first hydration shell of the wild-type and three quadruple mutant proteins. Hydrating water–water class: (■) apolar, (○) polar, (—) pure water.

ice-binding surface and type I THP thermal hysteresis activity.

DISCUSSION

This work was motivated by the ability of the RNM analysis of water hydration to reveal subtle but important changes in the water structure induced by polar and apolar solutes,[19–22] and by the desire to better understand the mechanism of type I THP activity and to see if a common mechanism could be proposed for different classes of THP protein. We performed extended MD simulations of type I antifreeze wild-type and three quadruple mutants in water using the CHARMM/TIP3P potential function and analyzed the protein hydration structure. The hydration structure was primarily analyzed in terms of the hydrating water–water "H-bond" angle, theta. The probability distribution of this angle, P(theta) is bimodal, and changes in the probability distribution were quantified by numerical integration of the two peaks, and expressed as a ratio. This ratio can be easily computed for the hydrating water over the entire protein surface or for any part of it, and compared to the ratio for bulk water. The results can be interpreted in terms of the apparent polarity of the solute using known low:high-angle population ratios of small polar and apolar solutes as a reference.

Applying this analysis to type I THP wild-type and three quadruple mutant proteins, we can draw several conclu-

sions. First, we note that the population ratios for apolar and polar hydrating water pairs averaged over the entire protein surface follow the expected trends based on polarity, and are similar for four proteins. However, the difference between polar and apolar protein group hydration is much smaller than the range seen in small molecule hydration. For example, compared to our highly polar solute standard (the potassium ion), the polar protein atoms' P(theta) distributions are not as distorted compared to bulk water, indicating that either water has a relatively weak interaction with these groups or the effect of neighboring polar and apolar groups on protein surface tend to cancel. Second, given that the angle population ratios may be interpreted as a reflection of polarity, looking at the entire protein surface, there is not much difference in average polarity among wild-type and three quadruple mutants, although these four proteins have different thermal hysteresis activities.

However, if we examine the structure of water in the ice-binding site we observe significant differences between active and inactive proteins, primarily with regard to polar atom hydration. For wild-type and active AAAA and VVVV mutants, water pairs solvating polar groups in the ice-binding site have a geometry very uncharacteristic of polar hydration. They are, in fact, more "ice-like" than water molecules hydrating apolar groups. Indeed, the population ratios are greater than those of the reference apolar solute
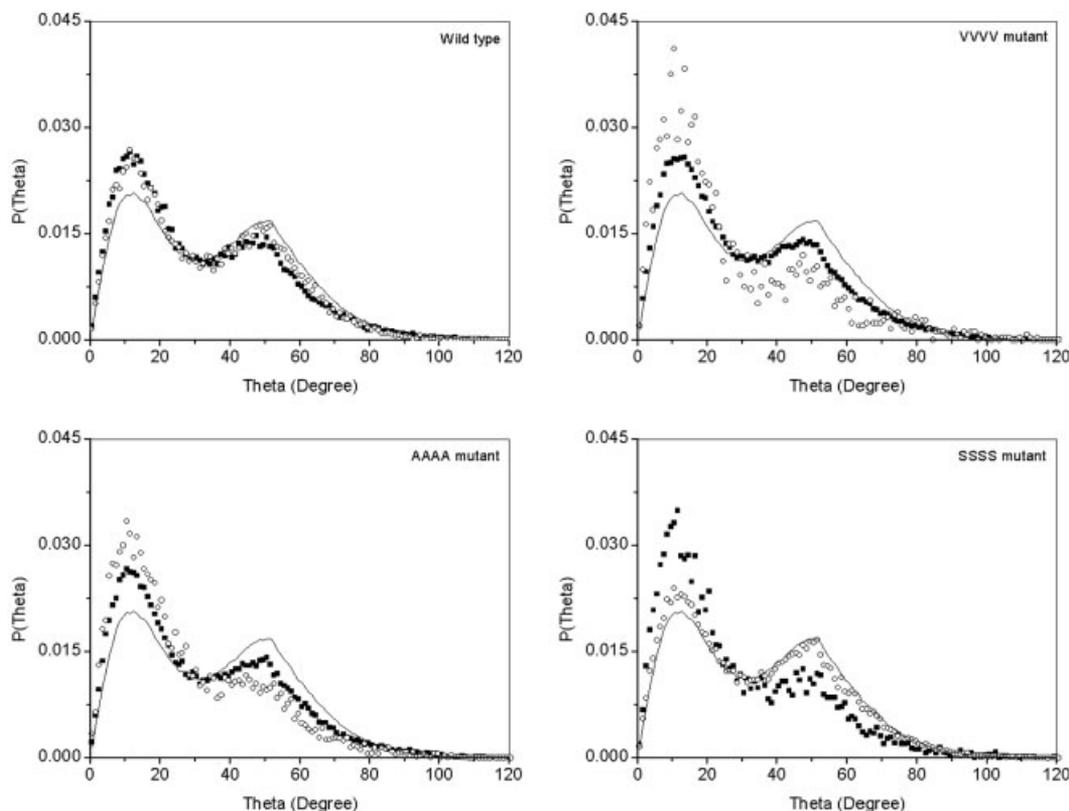
Fig. 7.   Water structure around residues 13 and 24 in type I THPs ice-binding sites. The water–water angle probability distributions for the first hydration shell of the wild-type and three quadruple mutant proteins. Hydrating water–water class: (■) apolar, (○) polar, (—) pure water.

methane (Fig. 8). In addition, apolar groups in the functional patch also exhibit more hydrophobic-like hydration (higher angle population ratios). Taken together, these results show that the hydration structure in the ice-binding site of the active proteins is, in general, more uniform across polar and apolar regions, and more "ice like." In structural terms, the hydration on the ice-binding surfaces of wild-type and active mutants can be described qualitatively as follows: there is formation of a water hydrogen-bond network with clathrate-like structure over the ice-binding face, which interacts at its edges with polar groups. We interpret this as the preference of the ice-binding surface, in terms of both affinity and specificity, for more ordered water and so favoring binding to the ice nuclei form of water over the liquid form. This effect depends on two things: the presence of apolar groups, and "apolar-like" hydration of neighboring polar groups, which have the ability to interact strongly with water. This conclusion is based on quantitative analysis of many water configurations averaged over extended simulations. Our interpretation in structural terms, and rationalization of the effect of different mutants is as follows.

For wild-type THP, the presence of both the hydrophobic methyl and hydrophilic hydroxyl groups in the Thr side chain maximizes the propensity for water hydration with a large low:high-angle ratio by presenting solvent-accessible polar and apolar groups in close prox-

imity. For the TTTT → SSSS mutation, deletion of methyl group leaves the polar hydroxyl group, which reverts to the standard polar hydration (enhanced high-angle or distorted, less ice-like hydration), which is not selective for binding to ice nuclei over bulk water. For the TTTT → VVVV mutation, the hydroxyl group is replaced with a methyl group. Despite the loss of the polar group from the side chain, there are still neighboring polar groups with low-angle (ice-like) hydration, in this case exposed backbone atoms (the amide and the carbonyl groups), which are close to the apolar side chain. A similar situation results with the TTTT → AAAA mutation: deletion of methyl and hydroxyl groups still leaves the apolar beta-carbon methyl and the neighboring backbone polar groups with low-angle (ice-like) hydration. The unique low water–water angle hydration pattern of active proteins is thus a direct consequence of the protein structure in the active site region, including the arrangement of polar/apolar groups, and the neighboring polar/apolar environment. However, it should be emphasized that the preceding rationalization is qualitative, and that it would be difficult to predict *a priori* the hydration pattern around different residues from their structure and known polarity. The systematic differences in hydration are only apparent from explicit solvent simulations, by sampling over many water configurations and using very sensitive struc-
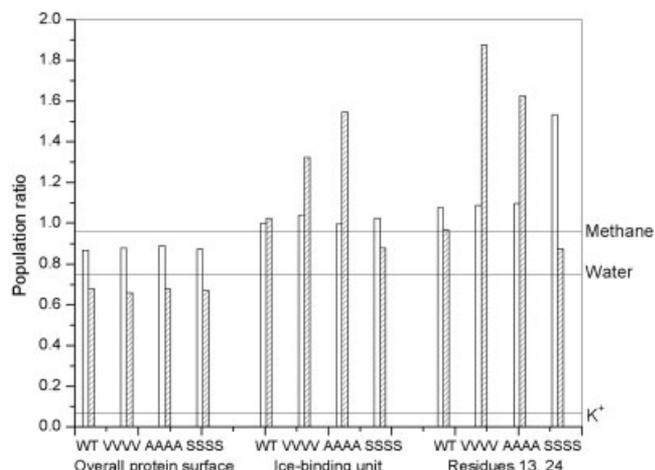
Fig. 8. Summary of P(theta) population ratios. The ratio of low-angle to high-angle populations in the water–water angle probability distributions for the entire protein surface, the ice-binding site, and the residues 13 and 24 in the ice-binding site. Unshaded bars, shaded bars indicate apolar and polar hydrating water–water classes, respectively. Ratios for pure water, and for hydration of methane and potassium are shown as horizontal lines for reference.

tural measures (e.g., angular distortions), typified by the RNM analysis.

THP activity seems to require the ice-binding site to play a dual role: maintain a somewhat apolar surface, but have a balance of polar and apolar groups to create hydration around polar groups with more ice-like structure. Apolar groups alone do not provide a strong enough interaction with water to drive ice binding, while polar groups alone favor less ice-like water. This is our conclusion both from this analysis of type I THP and from our previous analysis of type III THP.[23,26] Thus, we propose this as a common "mechanism" for THP proteins to preferentially bind ice nuclei that transcends the large differences in type I and type III THP structure, active-site size shape, and composition. In type III THP proteins there also seems to be a requirement for maintaining a flat ice-binding surface (large residue substitutions at position 16 reduce activity).[28,29] Flatness appears to be less important for type I THP as both AAAA and VVVV mutants have similar activities.

Regarding the progression of hydration structure shown in Figures 5–7, which refers to the hydration pattern over the whole protein, the binding surface, and the region in the ice-binding site immediately around residues 13 and 24, respectively, we can draw two conclusions: first, that the unique hydration pattern in active THP (polar group hydration that is more "ice-like" than that of apolar) is local and specific, confined to the ice-binding site. Second, that it is manifest at the residue–residue or residue–neighbor level, that is, it depends on residue context. The effect is masked by "normal" hydration when analyzed at the level of the entire protein surface (Fig. 5). Analysis at the individual residue level (Fig. 7) shows the trend, but less strongly than when the entire binding site is included in the analysis (Fig. 6). This is shown by the fact that only in Figure 6 do we see the effect. The requirement for

residue–neighbor or context effects is consistent with its origin: a combination of apolar and polar group modulation of water structure. Thus, the effect is partly due to apolar forces (shape, hydrophobicity), and partly electrostatic in nature with dipolar (hence, short-ranged) interactions. The unique hydration pattern in active THP is, however, local enough to account for the experimental observation that single point mutations can abolish activity.

There has been no generally accepted mechanism by which all classes of THP act. Several hypotheses based on the specific type of structural features and surface groups properties have been proposed.[1,3–16] A major argument among these hypotheses is whether THPs bind to the ice surface using polar or apolar groups. The calculations and analysis presented here reveal that both are required. We propose that active type I and type III THP proteins work as follows: upon ice crystals forming in liquid water, polar groups in the ice-binding site favor binding to this ice over liquid water due to their propensity for the more ordered hydration structure with ice-like water–water angles. In contrast, polar groups in the ice-binding site of the inactive mutant prefer binding to liquid water (with more distorted structure), which is present in large excess, over ice. In addition, the flatness of the ice-binding region and the protein–ice shape complementary could be a factor in enhancing affinity. We suggest that the major factor is that polar groups in the ice-binding surface must manifest apolar hydration, which depends upon neighboring apolar groups, implying a preference for ice-like water structure. This provides a solution to the affinity/specificity dilemma associated with using either polar groups (nominally with high affinity and low specificity) or apolar groups (nominally with low affinity and high specificity), and implies that both polar and apolar groups in close proximity are required. Finally, why doesn't a region that promotes more "ice-like" water nucleate ice formation? It may, but we suggest that any such nucleation remains attached to the protein and thus inhibited from growth in the same manner as an initially free ice nucleus that is bound by the protein.

CONCLUSIONS

MD simulations of type I THP wild-type and three quadruple mutants at Thr residues 2, 13, 24, and 35 in the ice-binding site were performed. The MD trajectories were used to analyze the solute-induced distortion of water structure within the framework of the RNM, which quantitatively describes hydrophobic or hydrophilic hydration. The water–water angular distribution function P(theta) revealed that the overall hydration structures of four proteins have standard features, apolar pairs with a higher low-angle population, while polar pairs have a lower high-angle population. In contrast, the water–water angular distribution function showed significant differences in the hydration structure of the ice-binding site between active and inactive proteins. For the wild-type and active AAAA and VVVV mutants, polar groups in the ice-binding site have a very ice-like hydration. In the inactive SSSS mutant, polar groups show standard polar-

like hydration. The more ice-like hydrating water structures formed on the ice-binding face of active THP implies that this protein surface has a high affinity and specificity for more ordered or ice-like water and thus for ice itself. The structure–function relationship suggests that the high affinity of type I THP binding for ice nuclei requires dual characteristics of the protein ice-binding surface, that is, polar groups in proximity to apolar groups, and having apolar-like hydration properties.

ACKNOWLEDGMENTS

REFERENCES

1. Sicheri F, Yang DSC. Ice-binding structure and mechanism of an antifreeze protein from winter flounder. Nature 1995;375:427–431.
2. Gronwald W, Loewen MC, Lix B, Daugulis AJ, Sonnchisen FD, Davies PL, Sykes BD. The solution structure of type II antifreeze protein reveals a new member of the lectin family. Biochemistry 1998;37:4712–4721.
3. Jia Z, DeLuca CI, Chao H, Davies PL. Structural basis for the binding of a globular antifreeze protein to ice. Nature 1996;384: 285–288.
4. Baardsnes J, Kondejewski LH, Hodges RS, Chao H, Kay C, Davies PL. New ice-binding face for type I antifreeze protein. FEBS Lett 1999;463:87–91.
5. Yang DSC, Sax M, Chakrabartty A, Hew CL. Crystal structure of an antifreeze polypeptide and its mechanistic implications. Nature 1988;333:232–237.
6. Knight CA, Cheng CC, DeVries AL. Adsorption of alpha-helical antifreeze peptides on specific ice crystal surface planes. Biophys J 1991;59:232–237.
7. Wen D, Laursen RA, Laursen RA. A model for binding of an antifreeze polypeptide to ice. Biophys J 1992;63:1659–1662.
8. McDonald SM, White A, Clancy P, Brady JW. Binding of an antifreeze polypeptide to ice/water interface via computer simulation. AIChE J 1995;41:959–973.
9. Cheng AKM, Merz J. Ice-binding mechanism of winter flounder antifreeze proteins. Biophys J 1997;73:2851–2873.
10. Haymet ADJ, Ward LG, Harding MM, Knight CA. Valine substituted winter flounder "antifreeze":preservation of ice growth hysteresis. FEBS Lett 1998;430:301–306.
11. Haymet ADJ, Ward LG, Harding MM. Winter flounder "antifreeze" proteins: synthesis and ice growth inhibition of analogs that probe the relative importance of hydrophobic and hydrogen-bonding interactions. J Am Chem Soc 1999;121:941–948.
12. Houston MEJ, Chao H, Hodges RS, Sykes BD, Kay CM, Sonnichsen FD, Loewen MC, Davies PL. Binding of an oligopeptide to a specific plane of ice. J Biol Chem 1998;273:11714–11718.
13. Chao H, Sonnichsen FD, DeLuca CI, Davies PL, Sykes BD. Structure–function relationship in the globular type III antifreeze protein: indentification of a cluster of surface residues required for binding to ice. Protein Sci 1994;3:1760–1769.
14. Sonnichsen FD, DeLuca CI, Davies PL, Sykes BD. Refined solution structure of type III antifreeze protein: hydrophobic groups may be involved in the energetics of the protein–ice interaction. Structure 1996;4:1325–1337.
15. Madura JD, Taylor MS, Wiezbicki A, Harrington JP, Sikes CS, Sonnichsen FD. The dynamics and binding of a type III antifreeze protein in water and on ice. J Mol Struct 1996;388:65–77.
16. Graether SP, DeLuca CL, Baardsnes J, Hill GA, Davies PL, Jia Z. Quantitative and qualitative analysis of type III antifreeze protein structure and function. J Biol Chem 1999;274:11842–11847.
17. Chen G, Jia Z. Ice-binding surface of fish type III antifreeze. Biophys J 1999;77:1602–1608.
18. Henn AR, Kauzmann W. Equation of state of a random network. Continuum model of liquid water. J Phys Chem 1989;93:3770–3783.
19. Madan B, Sharp K. Heat capacity changes accompanying hydrophobic and ionic solvation: a Monte Carlo and random network model study. J Phys Chem 1996;100:7713–7721.
20. Sharp KA, Madan B. Hydrophobic effect, water structure, and heat capacity changes. J Phys Chem B 1997;101:4343–4348.
21. Vanzi F, Madan B, Sharp K. Effect of the protein denaturants urea and guanidinium on water structure: a structure and thermodynamic study. J Am Chem Soc 1998;120:10748–10753.
22. Gallagher KR, Sharp K. A new angle on heat capacity changes in hydrophobic solvation. J Am Chem Soc 2003;125:9853–9860.
23. Yang C, Sharp KA. Mechanism of type III antifreeze protein action: a computational study. Biophys Chem 2004;109:137–148.
24. Brooks BR, Bruccoleri RE, Olafson BD, States DJ, Swaminathan S, Karplus M. CHARMM: a program for macromolecular energy, minimization and dynamics calculations. J Comp Chem 1983;4: 187.
25. MacKerell AD, Brooks B, Brooks CL, Nilsson L, Roux B, Won Y, Karplus M. CHARMM: the energy function and its parameterization with an overview of the program. In: Schleyer PvR, editor. The encyclopedia of computational chemistry, vol. 1. Chichester: John Wiley& Sons; 1998. p 271–277.
26. Gallagher KR, Sharp K. Analysis of thermal hysteresis protein hydration using the random network model. Biophys Chem 2003;105:195–209.
27. Gallagher KR. Electrostatic contributions to heat capacity changes and an analysis of thermal hysteresis protein hydration using the random network model. Philadelphia: University of Pennsylvania; 2002.
28. Yang DSC, Hon W-C, Bubanko S, Xue Y, Seetharaman J, Hew CL, Sicheri F. Identification of the ice-binding surface on a type III antifreeze protein with a "flatness function" algorithm. Biophys J 1998;74:2142–2151.
29. DeLuca CI, Davies PL, Ye Q, Jia Z. The effects of steric mutations on the structure of type III antifreeze protein and its interaction with ice. J Mol Biol 1998;275:515.